Supporting Information

Striemer et al. 10.1073/pnas.0905549106

SI Text

EC2. In addition to testing an 83-year-old healthy right-handed elderly male control (reported in the main manuscript), we tested an additional healthy 70-year-old right-handed male control under the same real-time and delay conditions. In the real-time condition, similar to EC1 reported in the main manuscript, EC2 demonstrated a significant sensitivity to the changing position of the obstacles 20 cm into the reach [$F(7, 112) = 43.95$, $P < 0.0001$] for both the left (in = 34.4 mm vs. out = 18.7 mm; $P = 0.003$) and right (in = −40.2 mm vs. out = −12.8 mm; $P < 0.0001$) visual fields (see Fig. S2 *A* and *B*).

For the delay condition, similar to the results from EC1 reported in the main text, at 20 cm into the reach, EC2 demonstrated a significant sensitivity to the changing position of the obstacles [$F(7, 75) = 41.06$, $P < 0.0001$]. Specifically, he demonstrated a significant sensitivity in his right visual field (in = −71.2 mm vs. out = −40.2 mm; $P < 0.0001$). In addition, for the left visual field, he demonstrated a clear trend toward a sensitivity to the position of the obstacles 20 cm into the reach (in = 23.7 mm vs. out = 10.4 mm; $P = 0.082$; see Fig. S2 *C* and *D*). In fact, for obstacles on the left, EC2 showed a sensitivity to their position that developed earlier in the reach. Specifically, the difference scores show a clear (and significant) separation between the two trajectories by 5 cm [one-sample *t test* $t(9) = 4.01$, $P = 0.003$] that continued to be significant until just beyond the obstacles (see Fig. S5*C*). In summary, these data clearly show that EC2's reaches are sensitive to the position of obstacles in the left and right visual fields for both the real-time and the delay conditions.

Young Controls. Finally, in addition to testing the two elderly male controls (EC1 reported in the main manuscript and EC2 reported above), we also tested six young healthy right-handed male controls (mean age = 26.5 years, range = 22–29 years) under the same real-time and delay conditions. Given that we tested a larger group of younger subjects, we only collected a total of 10 repetitions for each obstacle configuration condition for each Experiment.

For the real-time condition, similar to the two elderly controls, at 20 cm into the reach [$F(7, 35) = 25.77$, $P < 0.0001$], the young controls demonstrated a significant sensitivity to the position of the obstacles in the left (in = 2.7 mm vs. out = −5.26 mm; $P = 0.013$) and right visual fields (in = −33.7 mm vs. out = −19.7 mm; $P = 0.002$; see Fig. S3 *A* and *B*).

For the delay condition, similar to the two elderly controls, at 20 cm into the reach [$F(7, 35) = 30.19$, $P < 0.0001$], the young controls demonstrated a significant sensitivity to the changing position of the obstacles for both the left (in = 4.3 mm vs. out = −11.7 mm, $P = 0.001$) and right visual fields (in = −53.9 mm vs. out = −28.2 mm; $P = 0.004$; see Fig. S3 *C* and *D*).

In summary, both the young and elderly control subjects demonstrated sensitivity to the position of the obstacles in the left and right visual fields for the same real-time and delay conditions tested in the main experiment with patient CB.

Two-Obstacle and No-Obstacle Trials

Patient CB. In addition to the single obstacle trials (reported in the main text), we also included two obstacle trials in which the left obstacle was in and the right obstacle was out, and vice versa. In the context of the current experiment, these trials are hard to interpret given that CB was able to see one obstacle, but not the other. Thus, it is unclear whether the effects observed are driven by the position of the obstacle in the sighted (right) or blind (left) field. Nonetheless, CB was sensitive to the changing position of the obstacles (Fig. S1 *B* and *D*). Specifically in the real-time experiment, CB's reach end points were pushed further rightward when the left obstacle was in and the right obstacle was out (35.9 mm) compared to the opposite condition (18.3 mm; $P = 0.010$). For the delay experiment, the same comparison approached significance (left in, right out = 53.2 mm vs. left out, right in = 29.8 mm; $P = 0.023$); however, the effect was not significant after the Bonferroni correction (i.e., P must be 0.016).

Elderly Controls. EC1's reaches were also significantly influenced by the changing position of the obstacles (Fig. S1 *A* and *C*). That is, at 20 cm into the reach for both the real-time (left in, right out = −0.5 mm vs. left out, right in = −30.2 mm; $P < 0.0001$) and the delay experiments (left in, right out = −5.8 mm vs. left out, right in = −29.5; $P < 0.0001$), his trajectories were pushed significantly rightward when the left obstacle was in and the right obstacle was out compared to the opposite condition. EC2 demonstrated the same pattern of performance 20 cm into the reach. That is for the real-time (left in, right out = 24.9 mm vs. left out, right in = −4.5 mm; $P < 0.0001$) and the delay experiments (left in, right out = 28.2 mm vs. left out, right in = −0.7 mm; $P < 0.0001$) his reaches were also pushed significantly rightward when the left obstacle was in, and the right obstacle was out compared to the opposite condition (Fig. S4 *A* and *C*).

Young Controls. Finally, the group of young controls demonstrated the same pattern of performance as the elderly controls on the two obstacle trials for the real-time (left in, right out = −3.2 mm vs. left out, right in = −29.1 mm; $P = 0.001$) and delay experiments (left in, right out = 5.5 mm vs. left out, right in = −38.9 mm; $P < 0.0001$). That is, their reaches were pushed significantly rightward when the left obstacle was in, and the right obstacle was out compared to the reverse condition (Fig. S4 *B* and *D*).

No-Obstacle Trials. As was the case in previous studies (see references 4–8 in the main manuscript), we did not analyze no-obstacle trials statistically, although they are plotted alongside the two-obstacle trials in Figs. S1 and S4. We included the no-obstacle trials only so that the patient knew when he answered that he "saw nothing," there were actually trials in which "nothing" was the correct answer (to prevent the development of any odd strategies). It is important to emphasize that the reach trajectories in the no-obstacle trials should not be interpreted as some sort of "true baseline" with which to compare all of the other trajectories, because they are completely unconstrained reaches (in comparison to when obstacles are present). That is, the patient could reach anywhere (with any trajectory) on the table as long as he touched the target strip. There was no incorrect way of reaching. This makes the reach trajectories in these trials hard to interpret.

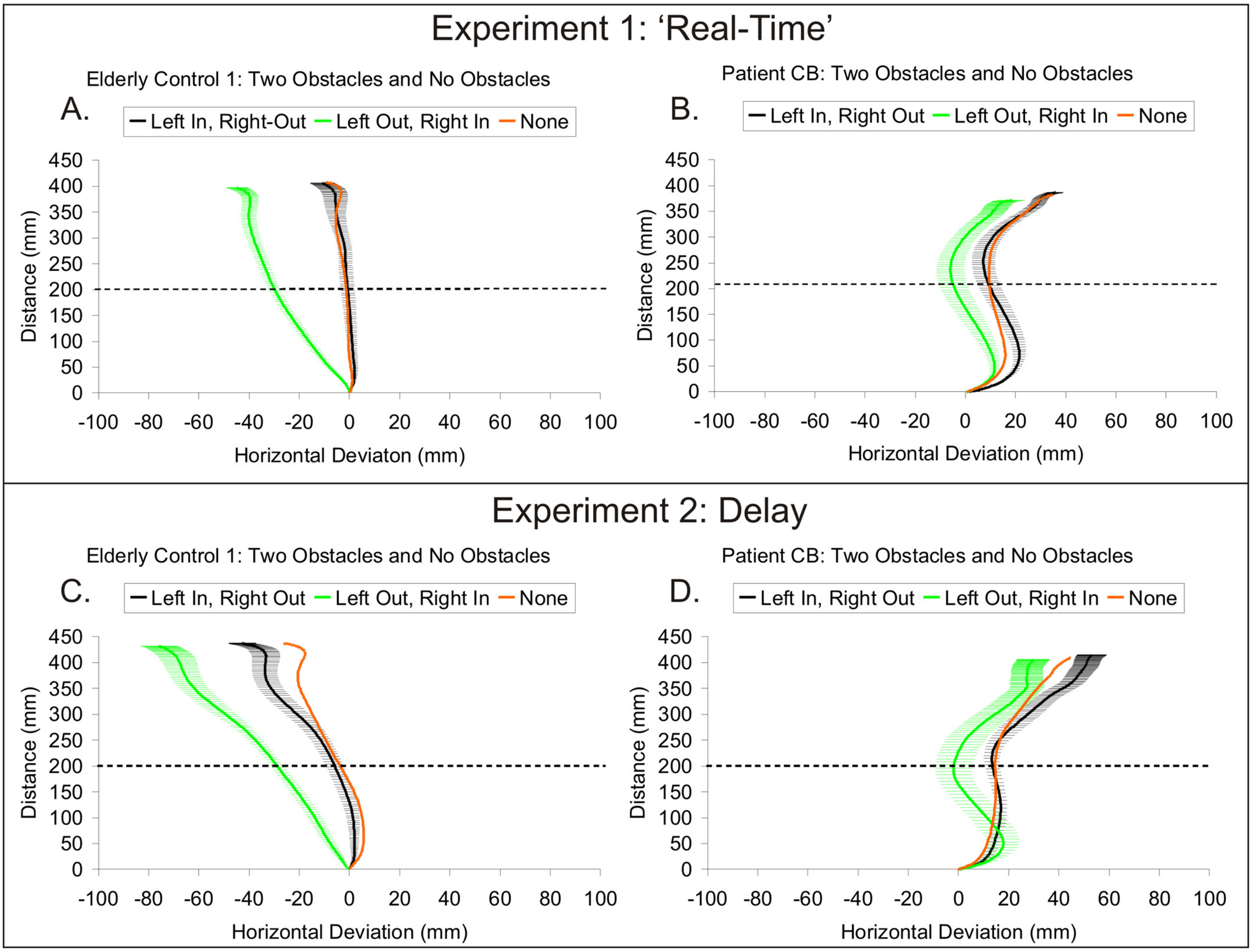

Fig. S1. Averaged spatial trajectories for two obstacle and no obstacle trials for EC1 and patient CB. Depicts averaged movement trajectories (± standard error) for EC1 (left) and patient CB (right) as a function of obstacle position (i.e., left in, right out vs. left out, right in). In addition, averaged trajectories from the no-obstacle trials are presented for comparison (standard error not plotted). Results from the real-time experiment are presented in the top panel (*A* and *B*), and results from the delay experiment are presented in the bottom panel (*C* and *D*). The x-axis depicts horizontal deviation in millimeters (mm), and the y-axis depicts reach distance in millimeters. Note that the x-axis has been magnified to illustrate the separation between trajectories. The dotted line represents the depth at which the obstacles were located (35 cm) from the reach start position (15 cm; i.e., 35 cm - 15 cm = 20 cm). Positive values refer to the right of midline, whereas negative values refer to left of midline. Note that patient CB's reaches were always directed to the right side of the target strip, the only part of the strip that he could see.

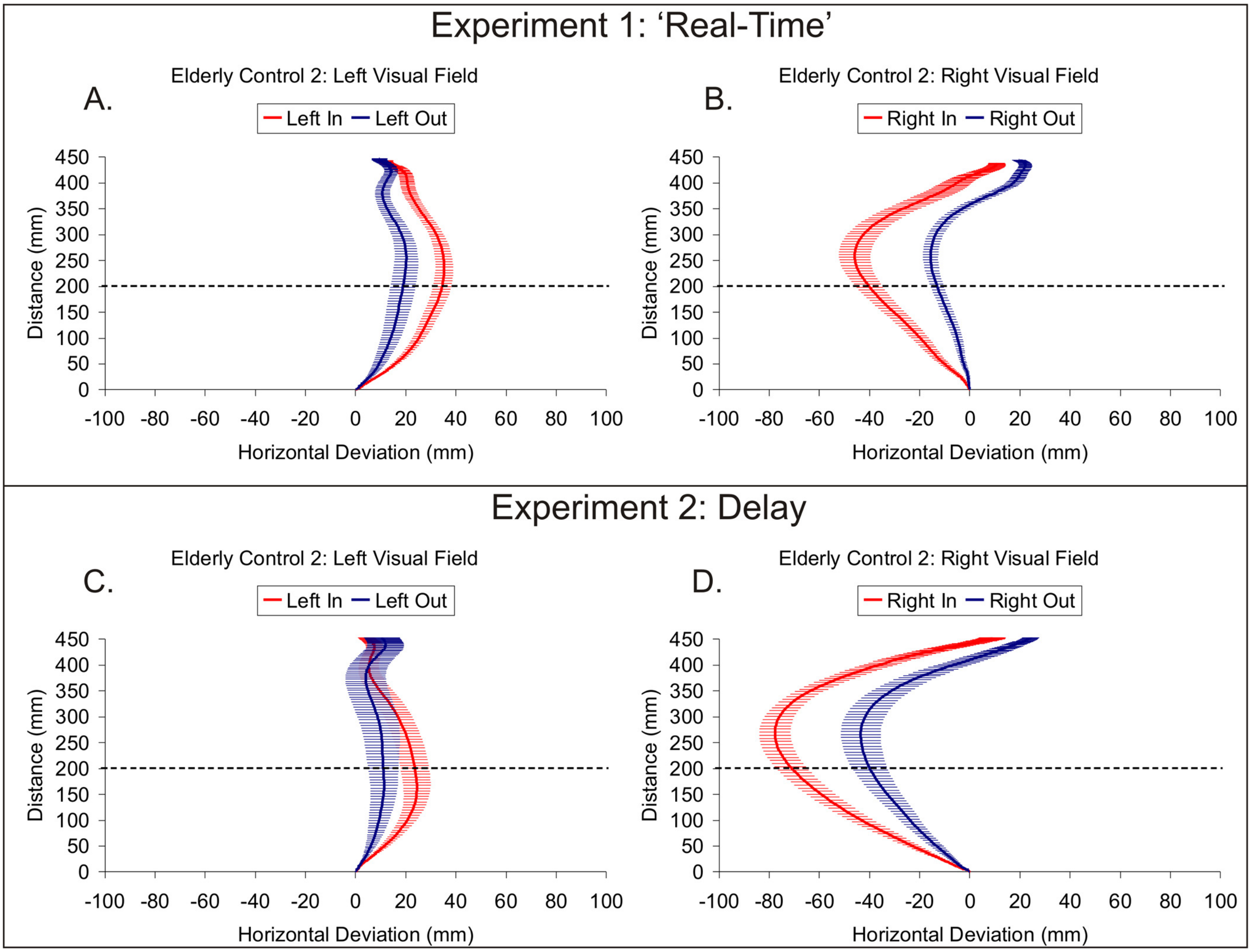

Fig. S2. Averaged spatial trajectories for EC2. Depicts averaged movement trajectories (± standard error) for EC2 as a function of obstacle position (i.e., in vs. out). Results from the real-time experiment are presented in the top panel (*A* and *B*), and results from the delay experiment are presented in the bottom panel (*C* and *D*). The x-axis depicts horizontal deviation in millimeters (mm), and the y-axis depicts reach distance in millimeters. Note that the x-axis has been magnified to illustrate the separation between trajectories. The dotted line represents the depth at which the obstacles were located (35 cm) from the reach start position (15 cm; i.e., 35 cm − 15 cm = 20 cm). Positive values refer to the right of midline, whereas negative values refer to left of midline.

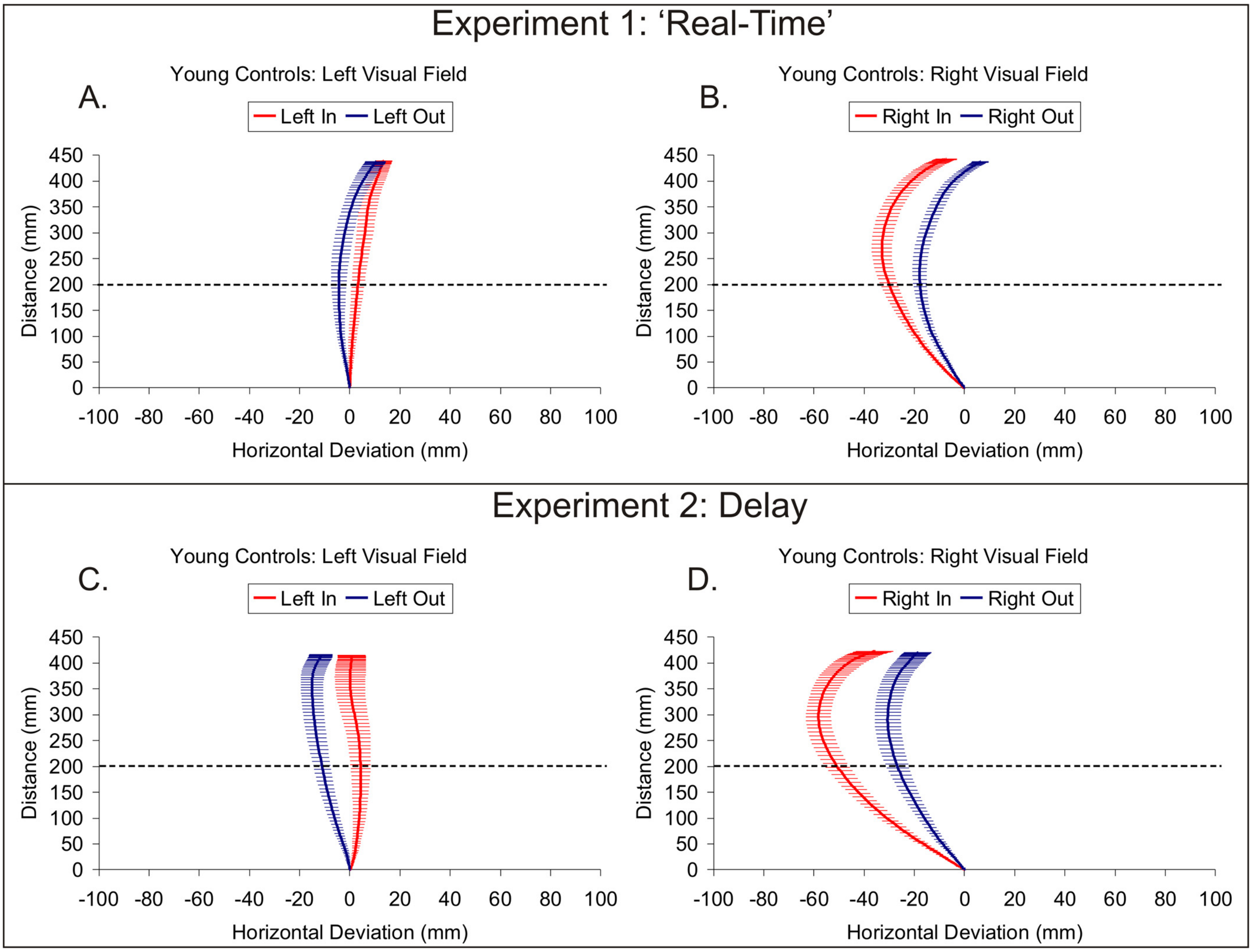

Fig. S3. Averaged spatial trajectories for the young controls ($n = 6$). Depicts averaged movement trajectories (± mean standard error) for the six young controls as a function of obstacle position (i.e., in vs. out). Results from the real-time experiment are presented in the top panel (*A* and *B*), and results from the delay experiment are presented in the bottom panel (*C* and *D*). The x-axis depicts horizontal deviation in millimeters (mm), and the y-axis depicts reach distance in millimeters. Note that the x-axis has been magnified to illustrate the separation between trajectories. The dotted line represents the depth at which the obstacles were located (35 cm) from the reach start position (15 cm; i.e., 35 cm - 15 cm = 20 cm). Positive values refer to the right of midline whereas negative values refer to left of midline.

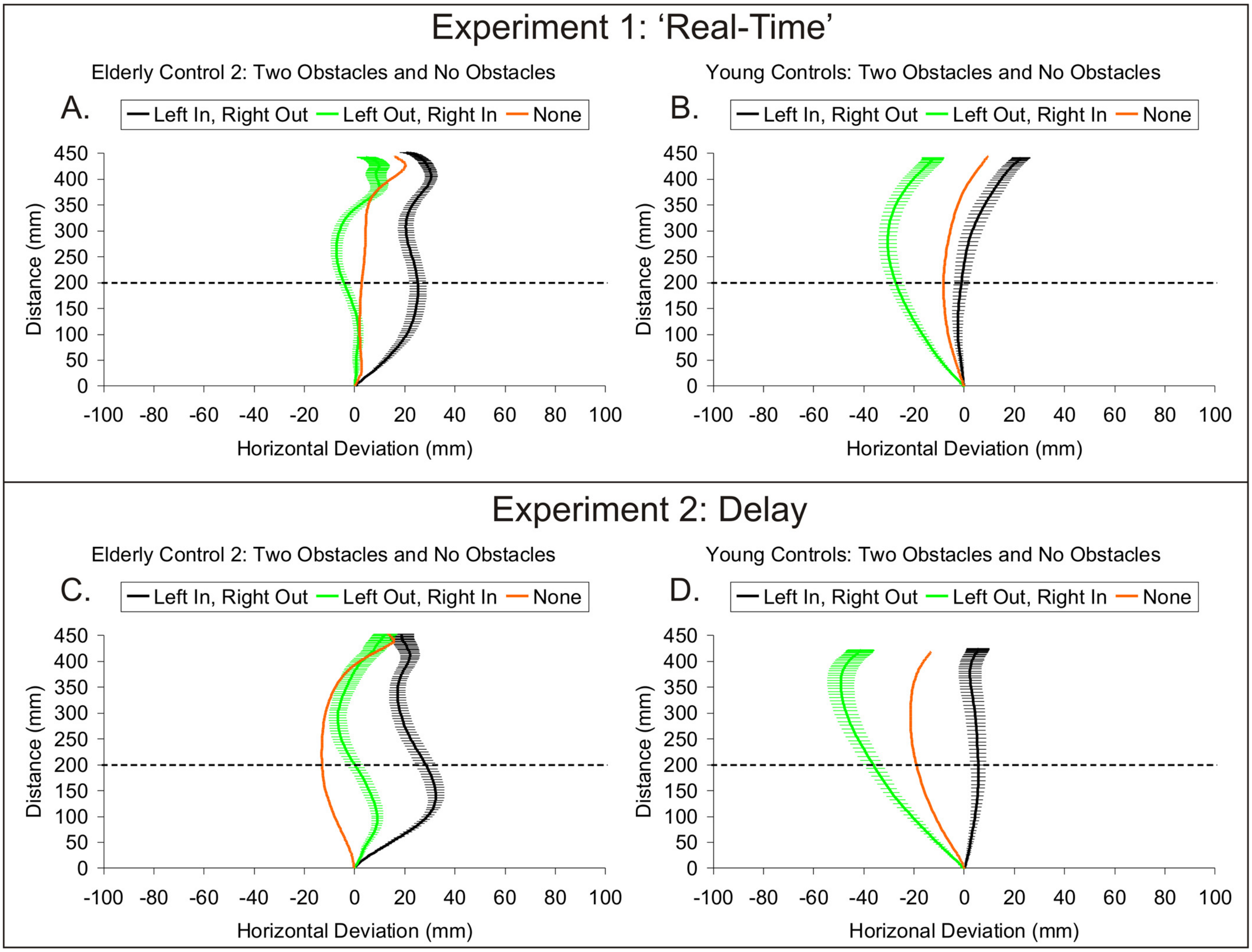

Fig. S4. Averaged spatial trajectories for two obstacle trials for EC2 and the young controls ($n = 6$). Depicts averaged movement trajectories (± standard error; mean SE for young controls) for EC2 (left) and the young controls (right) as a function of obstacle position (i.e., left in, right out vs. left out, right in). In addition, averaged trajectories from the no-obstacle trials are presented for comparison (standard error not plotted). Results from the real-time experiment are presented in the top panel (*A* and *B*), and results from the delay experiment are presented in the bottom panel (*C* and *D*). The x-axis depicts horizontal deviation in millimeters (mm), and the y-axis depicts reach distance in millimeters. Note that the x-axis has been magnified to illustrate the separation between trajectories. The dotted line represents the depth at which the obstacles were located (35 cm) from the reach start position (15 cm; i.e., 35 cm - 15 cm = 20 cm). Positive values refer to the right of midline, whereas negative values refer to left of midline.

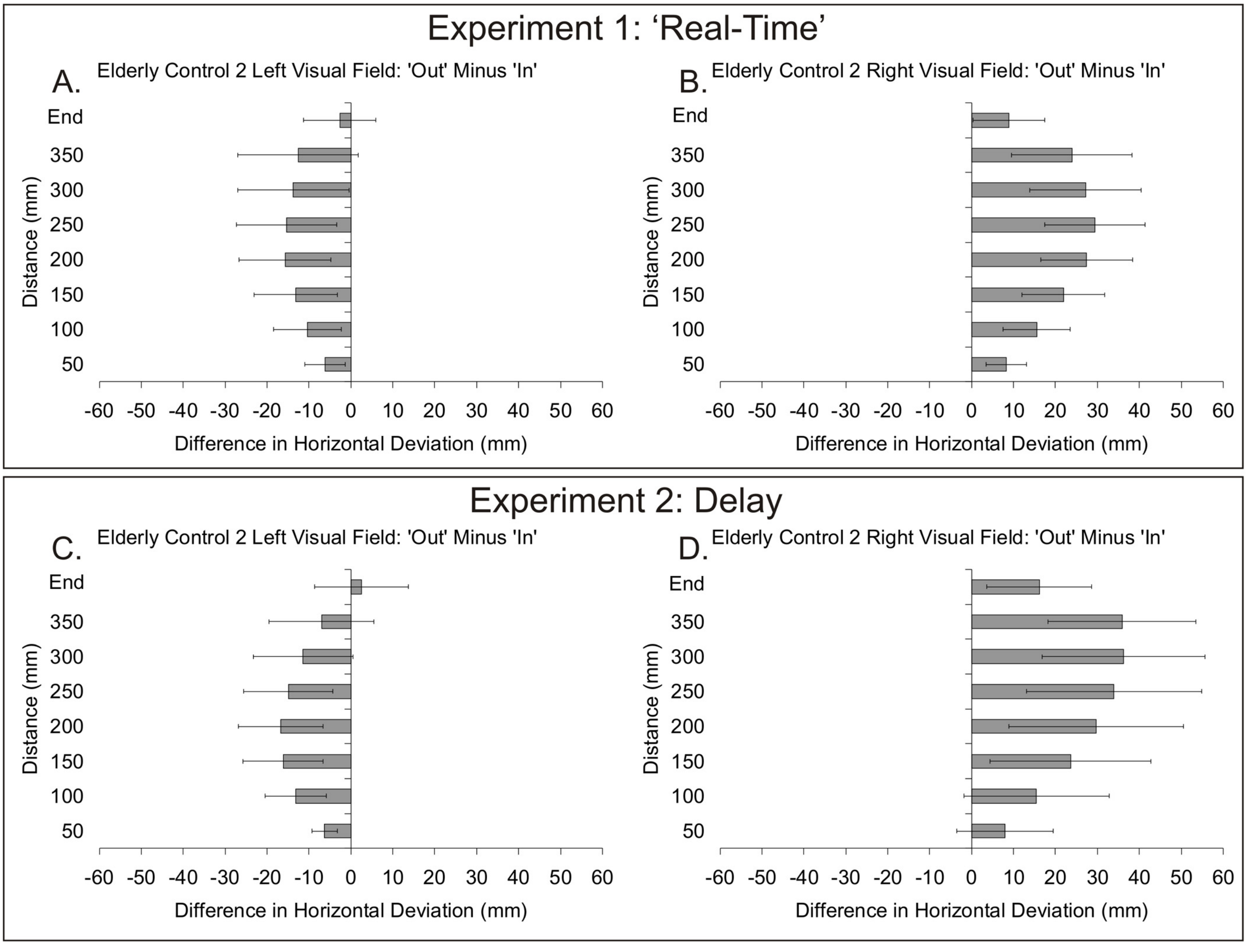

Fig. S5. EC2: Horizontal deviation difference scores (out minus in). Depicts mean difference scores (with 95% confidence intervals) between reach trajectories for the out and in conditions in 5-cm increments from 5 cm into the reach up to the end of the reach for EC2. The data from the real-time experiment are presented in the top panel, and the data from the delay experiment are presented in the bottom panel. Any condition in which the 95% confidence interval does not overlap zero indicates that the difference between the conditions is significantly different from zero. These data indicate that EC2's reach trajectories were significantly modulated by the position of the obstacles in both his left (*A*) and right (*B*) visual fields in the real-time condition. EC2's reaches were also sensitive to the position of the obstacles in the delay condition for both the left (*C*) and right (*D*) visual fields.

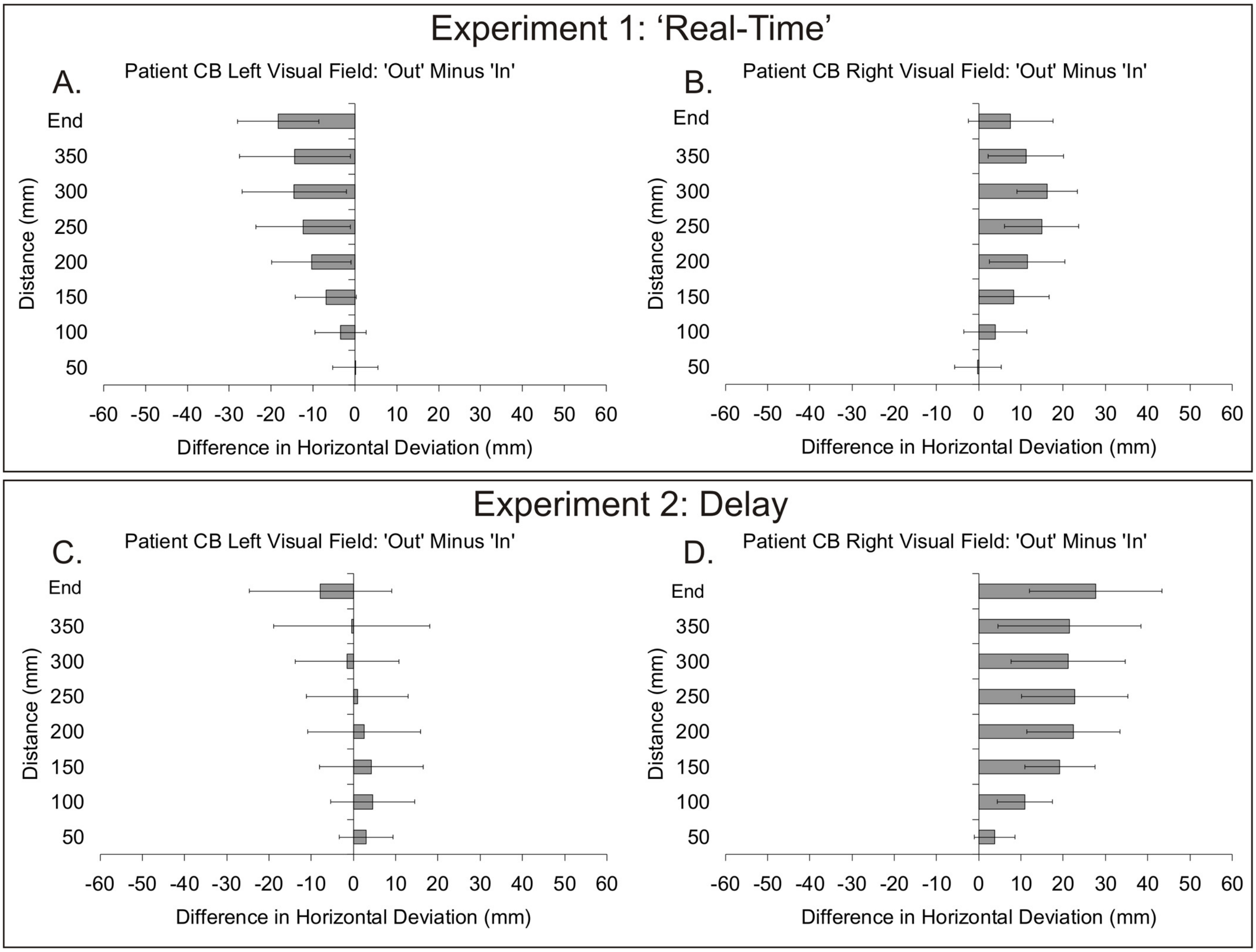

Fig. S6. Patient CB: Horizontal deviation difference scores (out minus in). Depicts mean difference scores (with 95% confidence intervals) between reach trajectories for the out and in conditions in 5-cm increments from 5 cm into the reach up to the end of the reach. The data from the real-time experiment are presented in the top panel, and the data from the delay experiment are presented in the bottom panel. Any condition in which the 95% confidence interval does not overlap zero indicates that the difference between the conditions is significantly different from zero. These data indicate that CB's reach trajectories for obstacles in his blind field (*A*) took longer to show a significant spatial separation compared to his sighted field (*B*). Importantly, these data also demonstrate that, while CB was clearly no longer sensitive to the position of obstacles in his blind field in the delay condition (*C*), he remained sensitive to the position of obstacles in his sighted visual field in the delay condition (*D*).

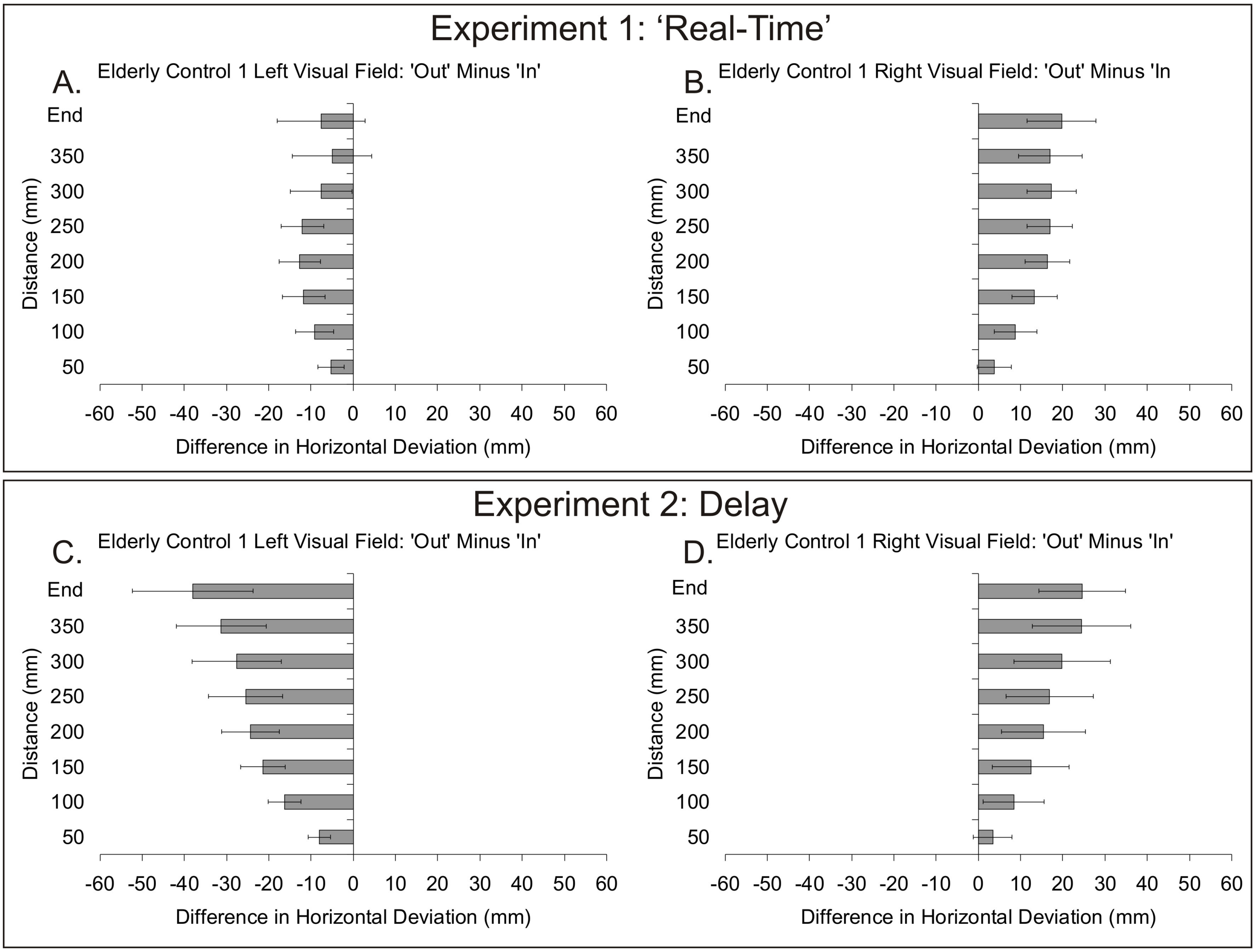

Fig. S7. EC1: Horizontal deviation difference scores (out minus in). Depicts mean difference scores (with 95% confidence intervals) between reach trajectories for the out and in conditions in 5-cm increments from 5 cm into the reach up to the end of the reach for EC1. The data from the real-time experiment are presented in the top panel, and the data from the delay experiment are presented in the bottom panel. Any condition in which the 95% confidence interval does not overlap zero indicates that the difference between the conditions is significantly different from zero.